Effective potentials for 6-coordinated Boron: a structural approach

W.-J. Zhu and C. L. Henley
LASSP, Cornell University, Ithaca NY 14853-2501

We have built an *ab-initio* LDA energy database with over 60 hypothetical extended structures of pure Boron, in each of which the coordination environment of each atom is equivalent. Focusing on eleven 6-coordinated structures, which are most relevant to the observed Boron phases, we deduce a nearest-neighbor-only 2-body interaction, refined by potentials that depend on angles and asymmetry within the local atomic environment. The resulting effective potentials describe the 6-coordinated structures with an average error of 0.1 eV/atom, and favor the environment most often seen in real Boron.

PACS. 34.20.Cf, 61.50.Lt, 71.20.Mq, 33.15.Dj

Boron as the prime candidate for a covalent quasicrystal has inspired activities in both experimental search and theoretical assessment, leading to identification of a new phase [1] and interests in nanotubes [2]. Accurate and fast structural energy estimators, capable of handling complex extended structures, can facilitate further investigations of these proposed structures, (through Monte-Carlo or Molecular Dynamics exploration), and might elucidate the structures of the unsolved or amorphous phases. While *ab-initio* methods have been used for comparing specific Boron structures [3,4], we seek a less computationally intensive effective theory, in the style of the environment-dependent effective interatomic potentials, which have successfully described Silicon bonding [5,6] but are not yet available for Boron.

The bonding behavior of Boron is unique among the elements and allows a number of complex structures. The atomic structures have been refined for only the metastable α_{12}, T_{50} and the stable β_{105} [7], while various complex phases remain unsolved [8]. Icosahedral clusters of various scales are present in all the known atomic arrangements, leading to unusual coordination environments and geometric patterns [9], quite unlike those in the well-studied covalent (e.g. Silicon) systems. In the case of the structurally simplest α_{12} phase, accurate electronic band structure [3], lattice dynamics studies and force models [10] all confirm the presence of 3-centered bonds, and the coexistence of soft metallic and strong covalent bonds both within and between icosahedra [11].

To design a classical potential (total energy function) that describes not only the uncommon bonding mechanisms and large-scale structural features, but also the unforeseen local configurations that may arise in quasicrystal models, we assume a local form $E_{total} = \sum_i E_i$, where E_i, the site energy of each atom, depends on its local atomic environment, as parametrized by bond distance, angles, and quantities involving more atoms.

Featuring the coordination number Z in environment-dependent energy functionals for Silicon, Tersoff [5] proposes Z-dependent bonds, while Bazant et al [6] formulate Z-dependent 2- and 3-body potentials to better capture the angular behavior. Making no assumptions for Boron, we investigate this type of description in its most general form of a Z-dependent N-body expansion,

$$E_i = \sum_j f(Z_i, r_{ij}) + \sum_{j\neq k} g(Z_i, r_{ij}, r_{ik}, \theta_{jk}^{(i)}) + ... \qquad (1)$$

where $j, k \neq i$ labels neighbors to atom i, r the magnitude of the interatomic distance, and $\theta_{jk}^{(i)}$ the angle formed by two neighbors j, k and center i.

In this letter we discuss a structural approach that naturally determines such potentials and allows straight forward assessment of the angular forces without assuming an analytic form. With an extensive energy database of the so-called "uniform" structures, constructed to have nearly identical bond lengths but large angular variation, we sample bonding mechanisms in widely different topologies and configurations. Focusing on 6-coordinated ($Z6$) structures, which are relevant to the real phases, we determine that their cohesive energies can be sufficiently described by $Z6$ potentials of the form

$$E_i^{Z6} = \sum_j f(r_{ij}) + \sum_{j\neq k} g(r_{ij}, r_{ik}, \theta_{jk}^{(i)}) + h(\xi_i) \qquad (2)$$

where j, k are now restricted to "nearest" neighbors of i, and the last term is a function of the site asymmetry ξ_i to be defined later.

In a "uniform" structure [12], all sites are geometrically equivalent by space-group symmetry operations, so that there is only one type of atomic environment occuring throughout the entire structure. We investigate those uniform structures in which all the nearest neighbor distances are equal (or nearly equal), so that angular effects are more clearly detected. Our database of over 60 uniform structures [13], spanning coordination numbers Z from 3 to 12, and exhibiting large angular variations for each Z, serves as a set of simple but topologically distinct representatives for different regions of configuration space. In fact, Boron compounds adopt certain of these structures as the sub-lattice for the Boron atoms [14].

$Z6$ coordinations are particularly important in Boron bonding, as they show up in 80% of the sites in β_{105}, and 50% in α_{12}. Therefore we focus now on the uniform $Z6$ structures, their bonding, and the effective potentials determined from them. Other coordinations are

discussed in [13]. In our list of $Z6$ structures (see Figure 1), besides the simple cubic (SC) and the triangular (tri) lattices, there are two 3D tilings: the simple cubic array of cuboctahedra (SC-co) and the diamond array of vertex-joint tetrahedra (T-lattice) [15]. From two $Z4$ planar lattices, the 3.4.6.4 ("i-dodec," for resembling a set of inter-penetrating dodecagons) and the 3.6.3.6 (Kagome), we get $Z6$ structures by stacking them with a separation of unit length (defined as the nearest neighbor distance.) There is also the Primitive Orthorhombic packing of icosahedra (PO-ico) [16] with inter-icosahedral distance set at unity.

We have constructed some novel Z6 structures as well. When we pucker a planar lattice, and mirror the operation in the next layer, each vertex gains one additional neighbor from either the layer above or below. So from the $Z5$ lattices $3^2.4.3.4$ (called σ) and the $3^3.4^2$ (called μ), we get the $P\sigma$ and $P\mu$ $Z6$ structures, ("P" for puckered). When we roll the triangular lattice into a single infinite tube with a circumference of 8 edges, we get the "tube-tri" structure [2]. Again, by rolling the $3^2.4.3.4$ (σ) lattice into a tube with a circumference shown by the dotted line in Figure 1-i, and arranging such tubes symmetrically in a square array (view along tube axes in Figure 1-j), we get the "tube-σ" structure, in which each atom has 5 neighbors on its own tube, and one more from a neighboring tube.

We show in Table I the distribution of "geometric quantities" found in the coordination environments of our $Z6$ structures, which will become helpful information in potential fitting. These consist of N_2 and N_3, the number of neighbors on the second and third shell, (at distances of $\sqrt{2}$ and $\sqrt{3}$, respectively), and frequencies of various "two-neighbor" angles, (which are formed at a central site and point toward two nearest neighbors). We also describe the asymmetry of these atomic environments, parametrized by

$$\xi = \frac{|\sum_j \mathbf{v}_j|}{(1/Z)\sum_j |\mathbf{v}_j|} \tag{3}$$

where j labels the nearest neighbors, and $\mathbf{v}_j$ the vector that points from the central atomic site to j. The denominator is just the average distance to nearest neighbors.

We perform *ab-initio* total energy calculation for each structure in our database [17], in the local density approximation [18] with extended norm and hardness conserving pseudo-potentials [19].

For each $Z6$ structure, the edge length "R" representing the nearest neighbor distance may be varied. In Figure 2, we present the cohesive energy (per atom) of the structure as a function of R in a range of physical interest. In the inset, where R scales from $1-5\mathring{A}$, we show the resulting single-well curves for three representative structures, SC, tri, and PO-ico [20]. The energy curves of i-dodec and Kagome fall closely onto the SC curve, and similarly the T-lattice onto the tri, and SC-co onto the PO-ico. Beyond $R = 3\mathring{A}$, all curves converge, and saturate toward the non-bonding limit.

In the main figure, we enlarge the $[1.6, 2.0]\mathring{A}$ region, (within which bond lengths from different structures all fall [2]), to clarify the difference among the wells of the energy curves. Our lowest energy $Z6$ structure is the PO-ico, a topologically different icosahedral packing. Within the next low energy structure, SC-co, is the cuboctahedron that has been compared to a distorted icosahedron using molecular orbitals theory [21]. For comparison, we include the lowest energy curve of the "ideal-α_{12}" phase, topologically same as α_{12} but with all nearest neighbor distances set equal.

To construct an effective theory, it is natural to start with a typical single-well 2-body potential, with nearest neighbors close to the minimum of the well, and further neighbors contributing at the tail of the well. This will not work for our $Z6$ energy curves. The large variation of N_2 and N_3 in Table I implies that the energy contribution from the further neighbors will lead to a large energy variation, on the order of the well-depth, among the structures. This contradicts the small energy differences among our energy curves in Figure 2. Indeed, numerical fittings with several single-well forms all substantiate this argument. We conclude that the 2-body potential has to be independent of N_2 and N_3, i.e. it must be essentially truncated after nearest-neighbor range.

Since we have shown the important result that the first term in Eq. 1 sums only the nearest neighbor j, our $Z6$ structures must have basically the same 2-body contribution of $6f(R)$ [22]. The energy differences among these structures would have to come from higher-order potentials. We choose the simple cubic energy curve to serve as the arbitrary reference in taking energy differences, and to give the function $f(x)$. We propose a 3-body potential that depends only on the two-neighbor angles. We also include a term $h(\xi)$ (compare Eq. 2) linear in ξ to test the degree of energy dependence on the asymmetry, which involves all Z neighbors. Allowing for dependence on the scale R, the cohesive energies (per atom) would lead to a set of linear relationships,

$$\Delta E_m(R) = \sum_a N_m(\theta_a) g(R, R, \theta_a) + c(R)\xi_m \tag{4}$$

where ΔE_m is the energy difference between the m-th structure and the reference, a labels the two-neighbor angles, N_m the number function per atom, and c the linear coefficient of ξ that depends on R.

A major problem in determining the functional form of the angular potential $g(R, R, \theta)$ is that the frequency of a particular angle θ_a cannot be varied independently of $\theta_{a'}$ to display its individual effect on the cohesive energy. Normally this problem is avoided by fitting to an assumed form [6], but for Boron, where angular behavior is still being explored, we have no analytic guidance as

to the form of this potential. However, the small number of distinct angles θ_a appearing among the structures in Table I helps to resolve this.

Since all nearest neighbor lengths are nearly equal, we can separate the R-dependence from the angular effects. The low number of distinct angles that appear in our $Z6$ structures allows us to determine the shapes of the angular potential without further assumptions. With the eleven $Z6$ structures and the data from Table I, we can solve numerically, in the least-squares sense, for $g(R, R, \theta_a)$ and $c(R)$, not assuming any functional form. Doing this at different R gives the radial dependence of g and c. The resulting fit, shown in Figure 3, suggests that the angular potential is linearly monotonically increasing. The R-dependence for each angle and $c(R)$ shows rapid decay. Similar potentials are found for Z5 structures [13].

Although the angular potential is obtained from the correlation of the number of angles with total energy, and not from measuring the direct effects each angle has on the site energy, this result is by no means trivial: for the potential value at each of the 7 angles is an independent parameter in the fit, yet the resulting $g(R, R, \theta)$ looks smooth as a function of (R, θ). Furthermore, we find that a separable form, i.e. $g(r_1, r_2, \theta) = \hat{g}(r_1)\hat{g}(r_2)A(\theta)$, is sufficiently determined, and a good approximation.

When we apply our potentials g and c to the $Z6$ "inverted-umbrella" environment [10] as found in the ideal-α_{12} structure, its site energy is 1.0 eV lower than that of the second best environment (PO-ico) among our structures. In fact, a Monte Carlo search among $Z6$ environments having all two-neighbor angles greater than 60°found no lower energy configurations. Since the effective potentials were constructed from environments all higher in energy, it is encouraging that they predict the realistic "inverted-umbrella" to be lowest in energy. Furthermore, our potential disfavoring 180° is in agreement with the tendency for Boron clusters to buckle in a hexagonally coordinated environment [2].

The angular and asymmetry potentials constructed so far can account for most of the 1-2 eV/atom energy variations among the $Z6$ structures, with an average error of 0.14 eV/atom in the bonding range. The energy ordering of our $Z6$ structures are mostly retained by the potentials. Although we still need to treat other Z's, and test cases when not all neighbors are at the same distance, we see a promising start in the local potential description for the general Boron system, without many-body terms involving, e.g. all the atoms in an icosahedron.

We thank M. Teter, D. Allen, J. Charlesworth for providing code and support in the LDA calculation, A. Quandt, M. Sadd for comments, K. Shirai, P. Kroll and R. Hoffman for discussion. This work is supported by DOE grant DE-FG02-89ER45405.

[1] M. Takeda, et al. Phys. Rev. B **48** 13159 (1993).
[2] I. Boustani, A. Quandt, and P. Kramer, Europhys. Lett., **36**, 583 (1996); I.Boustani, et al. Europhys. Lett., **39**, 527 (1997); I. Boustani, Surface Sci. **370**, 355(1997); Phys. Rev. B **55**, 16426 (1997).
[3] S. Lee, D.M. Bylander, and L. Kleinman, Phys. Rev. B **42**, 1316 (1990); S. Lee, et al. Phys. Rev. B **45**, 3248 (1992); I. Morrison, et al. Phys. Rev. B **45**, 10872 (1992).
[4] High pressure boron phases had previously been studied by C. Mailhoit, et al. Phys. Rev. B **42**, 9033 (1990).
[5] J. Tersoff, Phys. Rev. Lett. **56**, 632 (1986); Phys. Rev. B **37**, 6991 (1988); **38**, 9902 (1988).
[6] M. Z. Bazant and E. Kaxiras, Phys. Rev. Lett. **77**, 4370 (1996); M. Z. Bazant, et al. Phys. Rev. B **56**, 8542 (1997).
[7] The commonly known β_{105} is re-identified as β_{320}, in G. A. Slack, et al. J. Solid State Chem. **76** 52 (1988), and the tetragonal B_{50} is calculated to be unstable [3].
[8] J. Donohue, *The structures of the elements* (Wiley, New York, 1974).
[9] J. L. Hoard and R. E. Hughes, in *The Chemistry of Boron and its Compounds*, edited by E. L. Muetterties (John Wiley & Sons, New York, 1967), p. 40.
[10] K. Shirai, Phys. Rev. B **55** 12235 (1997); J. Solid State Chem. **133**, 215 (1997).
[11] H. C. Longuet-Higgins and M. de V. Roberts, Proc. Roy. Soc. London, Ser. **A 230**, 110 (1955).
[12] A. F. Wells, *Three-dimensional nets and polyhedra* (John Wiley & Sons, New York, 1977).
[13] W.-J. Zhu and C. L. Henley, unpublished.
[14] D. B. Sullenger and C. H. L. Kennard, Sci. Am. p. 66, July 1966.
[15] M. O'Keefe and B.G. Hyde, *Crystal Structures* (Mineralogical Society of America, Washington, D.C. 1996), p. 240, 276.
[16] S. Lee, et al. Phys. Rev. B **46**, 12121 (1992).
[17] We use all planewaves with kinetic energy up to 54.5 Ry. The Brillouin zone is sampled with a k-point density of at least $(16.3\mathring{A}^{-1})^3$. Band structure energies are converged to within 10^{-6} Ry in each calculation. The convergence with respect to k-point density shows a precision of 0.03 eV for energy comparison among different structures.
[18] M. C. Payne, et al. Rev. Mod. Phys. **64**, 1045 (1992).
[19] M. Teter, Phys. Rev. B **48**, 5031 (1993).
[20] For each structure, with unit length defined as $1.631\mathring{A}$, the shortest bond length found in the α_{12} phase, we sampled 10 energy data points at increment of 2% dilation within the single-well region, and then at total dilations of 0.7, 0.8, 0.9, 1.5, 2.0, 3.0 and 5.0. We present here the spline fitted curve.
[21] D. W. Bullett, in *Boron-rich Solids*, edited by D. Emin, et al. (American Institute of Physics, New York, 1986).
[22] $P\sigma$ has 4 nearest neighbors at 1.03108 R, and tube-σ has 2 at 1.0072 R and 1 at 1.0256 R. These corrections are accounted for in the 2-body energies.

TABLE I. Local environments of $Z6$ structures.

Structure	N_2	N_3	$N(\theta_a)$							ξ
			60°	90°	108°	120°	135°	150°	180°	
SC	12	8	0	12	0	0	0	0	3	0
tri	0	6	6	0	0	6	0	0	3	0
SC-co	7	6	2	7	0	2	4	0	0	0.586
T-lattice	0	12	6	0	0	6	0	0	3	0
i-dodec	10	6	1	10	0	1	0	2	1	0.732
Kagome	8	4	2	8	0	2	0	0	3	0
PO-ico	1	10[a]	5	1	7	0	0	2[b]	0	1.854
$P\sigma$ [c]	4[b]	12[a]	3	3[b]	4[b]	1[b]	2[b]	2[b]	0	0.263
$P\mu$	5[b]	10[a]	3	4	3[b]	2	2[b]	0	1	0.771
tube-tri	0	6[a]	6	0	0	6[b]	1	0	2[d]	1.163
tube-σ [c]	5[b]	7[a]	3	5[b]	2[b]	2	0	3[b]	0	0.936

[a]Neighbors between the second and third shells, occuring at various distances, are binned in N_3.
[b]These bins have tolerance of 0.14 unit distance, or 6°in angle.
[c]Nearest neighbors not all at unit distance [22].
[d]This is at 169°.

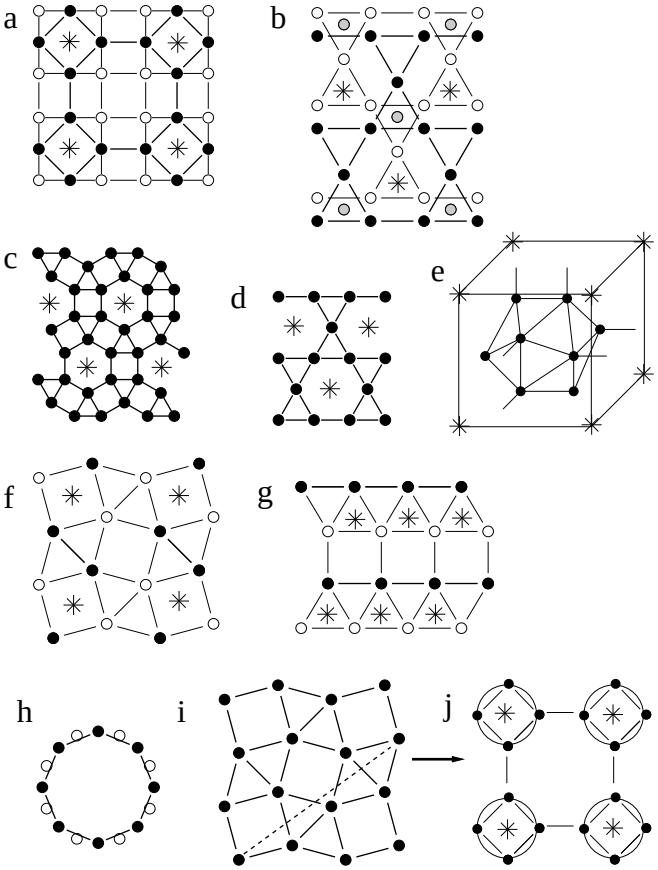

FIG. 1. The less familiar $Z6$ structures, with Bravais lattice indicated by $*$. For structures in layer form, • are nearest to the viewer, and ○ furthest. (a) SC-co (• • ○ stacking), (b) T-lattice, in which the Kagome layer has an (ABC) type stacking, (c) i-dodec, (d) Kagome, (e) PO-ico, (f) $P\sigma$, (g) $P\mu$, (h) tube-tri, (i)&(j) tube-σ (see text).

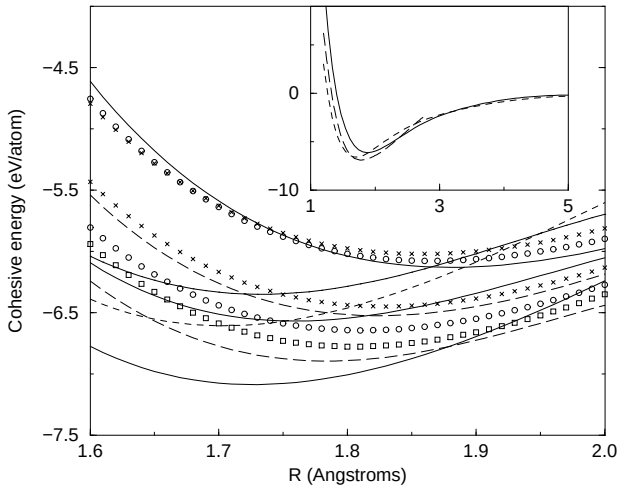

FIG. 2. Cohesive energy $E_i(R)$ for $Z6$ structures. In the inset, the three representative structures are SC (line), tri (short-dash), and PO-ico (long-dash). The region showing the energy wells is magnified in the main figure. The structures are, in order of lowest to highest energy at $R = 1.8\mathring{A}$, ideal-α_{12} (line), PO-ico (long-dash), SC-co ($\Box$), tube-σ ($\circ$), T-lattice (line), P-μ (long-dash), tri (short-dash), P-σ ($\times$), tube-tri (line), SC (line), i-dodec ($\circ$), and Kagome ($\times$).

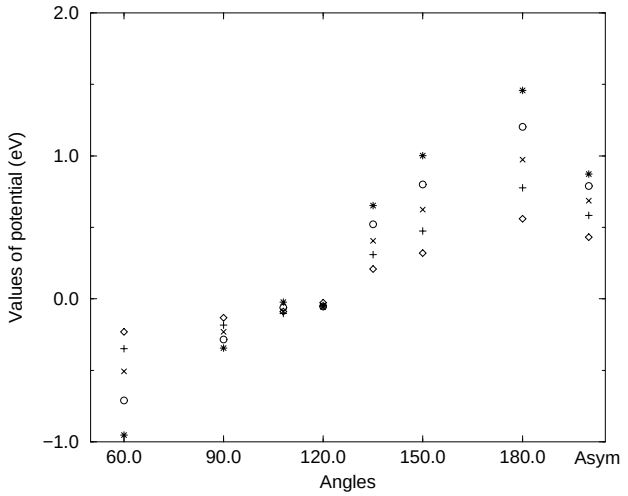

FIG. 3. Angular and asymmetry potentials. The angles take on values from 60°to 180°. Data in the "Asym" column signifies the coefficient $c(R)$ in the asymmetry potential. The $g(R, R, \theta)$ and $c(R)$ are illustrated by symbols $\{*, \circ, \times, +, \diamond\}$, corresponding to $R = \{1.6, 1.7, 1.8, 1.9, 2.0\}\mathring{A}$.